

Determination of the crack-tip toughness in silicon nitride ceramics

S. Fünfschilling · T. Fett · M. J. Hoffmann ·
R. Oberacker · H. Jelitto · G. A. Schneider

Received: 4 September 2008 / Accepted: 24 November 2008 / Published online: 9 December 2008
© Springer Science+Business Media, LLC 2008

Fracture in most ceramic starts from natural cracks with sizes a_0 in the order of a few 10 μm introduced during the processing of these materials. A crack in a component starts to propagate when the externally applied stress intensity factor K_{appl} exceeds the so-called crack-tip toughness K_{10} . In the absence of an increasing crack growth resistance, the strength σ_c is exclusively governed by K_{10} according to

$$\sigma_c = \frac{K_{10}}{Y\sqrt{a_0}}, \quad Y \cong 1.3 \quad (1)$$

Many ceramic materials exhibit the effect of an increasing crack growth resistance during crack extension Δa , i.e. a rising R-curve with $K_R = f(\Delta a)$ (Fig. 1a). In cases of a moderately rising R-curve, Eq. 1 remains valid. Only in cases of strongly rising R-curves, the strength is affected. For materials with a sufficiently steep R-curve, stable crack extension follows under increasing load. Failure of the component then occurs when the so-called tangent condition is fulfilled, i.e. when the slope of the applied stress intensity factor $K_{\text{appl}}(a)$ and the R-curve $K_{\text{IR}}(a)$ are identical

$$K_{\text{appl}} = K_R, \quad \frac{dK_{\text{appl}}}{da} = \frac{dK_R}{da} \Rightarrow \sigma_c = f(a_0, K_R) \quad (2)$$

The stress intensity factor at which (2) is fulfilled is called “fracture toughness” K_{Ic} , which is introduced in Fig. 1a as a triangle.

It follows from (2) that failure behavior in the presence of R-curve behavior can be assessed only if both the shape of the initial R-curve and the crack-tip toughness K_{10} are known.

For high-strength applications, silicon nitride ceramics are of highest importance. Therefore, many R-curve measurements on this material class were carried out in literature with the general result of the occurrence of very steep R-curves. Nevertheless, only a few data for K_{10} are available. The main reason of this lack is the fact that the range of Δa in which K_R rises from K_{10} to the saturation value K_{Rmax} (Fig. 1a) is extremely short and, consequently, an extrapolation of the R-curve to $\Delta a = 0$ is hardly possible.

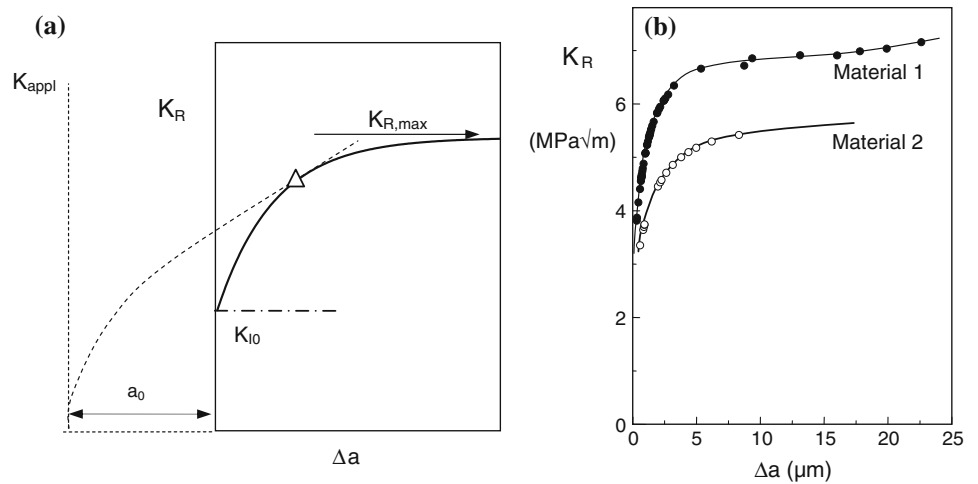
An independent method to measure K_{10} is the evaluation of crack-opening displacements (COD). Measurements by Pezzotti et al. [1] on an Al_2O_3 and Y_2O_3 containing Si_3N_4 produced via gas-pressure sintering yielded $K_{10} = 2.7 \text{ MPa}\sqrt{\text{m}}$. From COD for a sintered reaction-bonded silicon nitride (SRBSN) by Kouna Njiwa et al. [2], a range of $1.45 \text{ MPa}\sqrt{\text{m}} \leq K_{10} \leq 1.95 \text{ MPa}\sqrt{\text{m}}$ could be concluded. For yttria doped material used in the present study, Kruzic et al. [3] determined $K_{10} = 1.4 \text{ MPa}\sqrt{\text{m}}$ by use of a Raman spectroscopy method. In this article, two Si_3N_4 ceramics containing ($\text{Y}_2\text{O}_3, \text{MgO}$) and ($\text{Y}_2\text{O}_3, \text{Al}_2\text{O}_3$) are studied by COD measurements.

Material (I) was a silicon nitride which was consolidated in a two-step sintering process. The powder mixture of silicon nitride, 5 wt% Y_2O_3 , and 2 wt% MgO was prepared by attrition milling in isopropanol and afterwards dried and sieved. Greenbodies ($45 \times 64 \times 6 \text{ mm}$) were uniaxially pressed and subsequently cold isostatically densified. The

S. Fünfschilling · T. Fett (✉) · M. J. Hoffmann · R. Oberacker
Institut für Keramik im Maschinenbau, Universität Karlsruhe,
Karlsruhe, Germany
e-mail: theo.fett@ikm.uni-karlsruhe.de

H. Jelitto · G. A. Schneider
Institut für keramische Hochleistungswerkstoffe, Technische
Universität Hamburg-Harburg, Hamburg, Germany

Fig. 1 **a** Schematic of an R-curve $K_R(\Delta a)$ with the crack-tip toughness K_{I0} as the starting value (triangle: failure condition given by Eq. 2). **b** R-curve of the yttria-containing silicon nitrides for small crack extensions



samples were sintered in a hot isostatic press. In the first step with a low N_2 pressure of 1 MPa, the sample was sintered to achieve closed porosity at a temperature of 1750 °C. Full density was achieved in the HIP step at an N_2 pressure of 20 MPa and a temperature of 1800 °C. Material (II) is a commercial silicon nitride containing Y_2O_3 and Al_2O_3 (SL200BG, CeramTec, Plochingen, Germany).

The R-curves for these materials were measured in a very stiff test device as described in Ref. [4]. Four-point bending tests were carried out on notched bars of dimensions $W = 4$ mm, $B = 3$ mm with the support rollers distances of 10 and 20 mm. The procedure used for silicon nitride was demonstrated in Ref. [5] for a specimen of material (1) with a notch length $a_0 = 2.75$ mm and notch root radius of $R = 6.2$ μm introduced with the razor blade procedure.

Incremental stable crack growth is achieved automatically by a computer aided control system. In the very first part of the tests, the R-curve was determined by

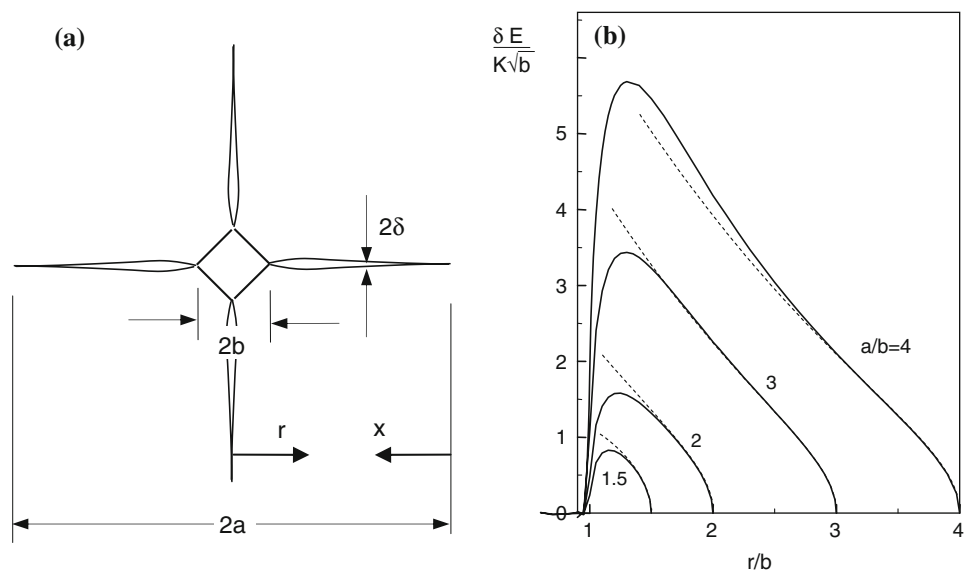
compliance evaluation including the effect of the notch on stress intensity factor and compliance.

Figure 1b shows the results for the first microns of crack propagation. It can be seen that the R-curves raise very steeply reaching saturation already after a few μm crack extension. A saturation value of about $K_R \approx 7$ MPa√m for material (I) is reached even after 10 μm crack propagation.

For the determination of the starting point of the R-curve, K_{I0} , Vickers indentation tests were performed on polished surfaces with an indentation load of 98.8 N with a dwelling time of 15 s. Before the indentation tests, the surfaces were polished up to 1 μm diamond slurry and afterwards slightly plasma etched for 1 min with a 4:2 $CF_4:O_2$ gas mixture.

Since the semi-elliptical crack shape of Vickers cracks develops in the unloading phase, these cracks are characterized by the condition of $K = K_{I0}$ at the crack tip after load removal. Figure 2a illustrates the quadratic impression

Fig. 2 **a** Vickers indentation (geometric parameters) and **b** crack opening displacements: comparison of the analytical solution (solid curves) with the approximation Eqs. 1–3 (dashed curves)



of the indenter with diagonal $2b$ and the cruciform semi-circular crack system with diameter $2a$. The total crack opening 2δ has to be measured under the scanning electron microscope (SEM).

In order to determine the actually present stress intensity factor after unloading, a relation between COD and stress intensity factor is necessary. An analytical solution for the COD of Vickers indentation cracks was given in Ref. [6].

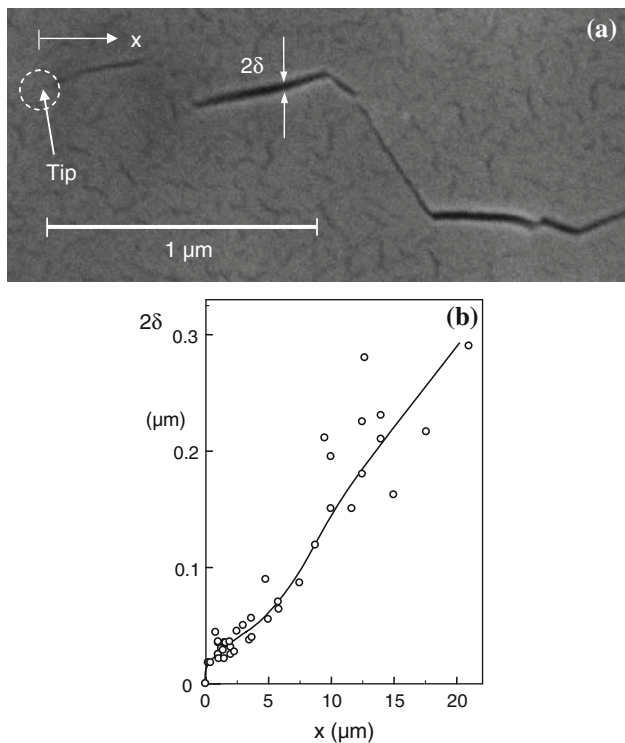
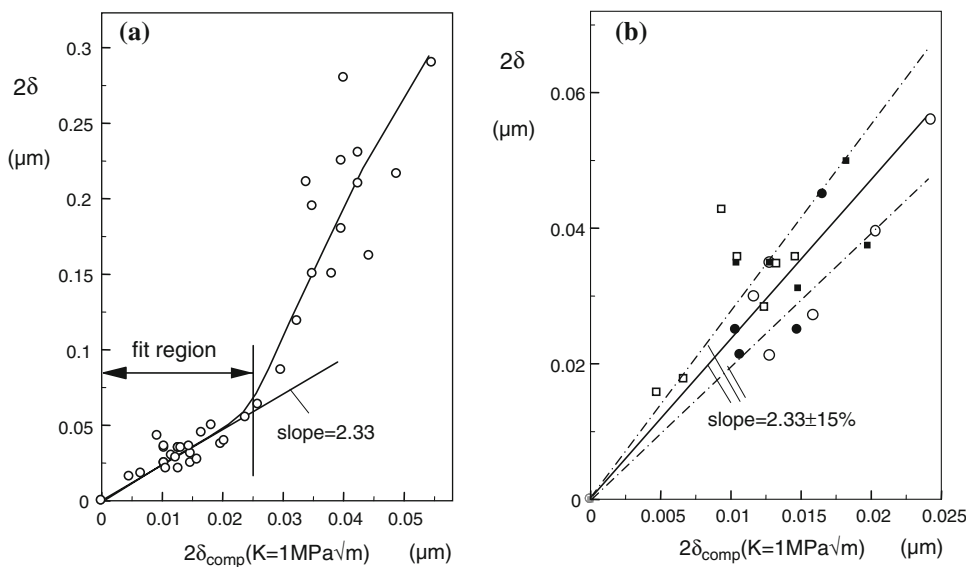


Fig. 3 **a** SEM image of the near-tip region of a Vickers indentation (material I) and **b** near-tip opening for a Vickers indentation crack introduced in a non-etched surface

Fig. 4 **a** Measured CODs plotted versus the displacements computed by Eqs. 3–5 for a stress intensity factor of $K = 1 \text{ MPa}\sqrt{\text{m}}$, and **b** near-tip data; *solid straight line*: least-squares fit (the *dash-dotted straight lines* border the region including 66% of the data points)



This solution is shown in Fig. 2b by the solid curves. In Ref. [7], a simplified series expansion for the displacements was proposed. For $a/b > 1.4$, this approximation is represented by a series expansion. Considering the leading terms exclusively, it holds

$$\frac{\delta}{K} = \frac{\sqrt{b}}{E'} \left(\sqrt{\frac{8x}{\pi b}} + A_1 \left(\frac{x}{b}\right)^{3/2} + A_2 \left(\frac{x}{b}\right)^{5/2} \right) \tag{3}$$

with the coefficients A_1 and A_2 fitted as

$$A_1 \cong 11.7 \exp[-2.063(a/b - 1)^{0.28}] - \frac{0.898}{a/b - 1}, \tag{4}$$

$$A_2 \cong 44.5 \exp[-3.712(a/b - 1)^{0.28}] - \frac{1}{(a/b - 1)^{3/2}} \tag{5}$$

and the effective modulus E' defined usually by

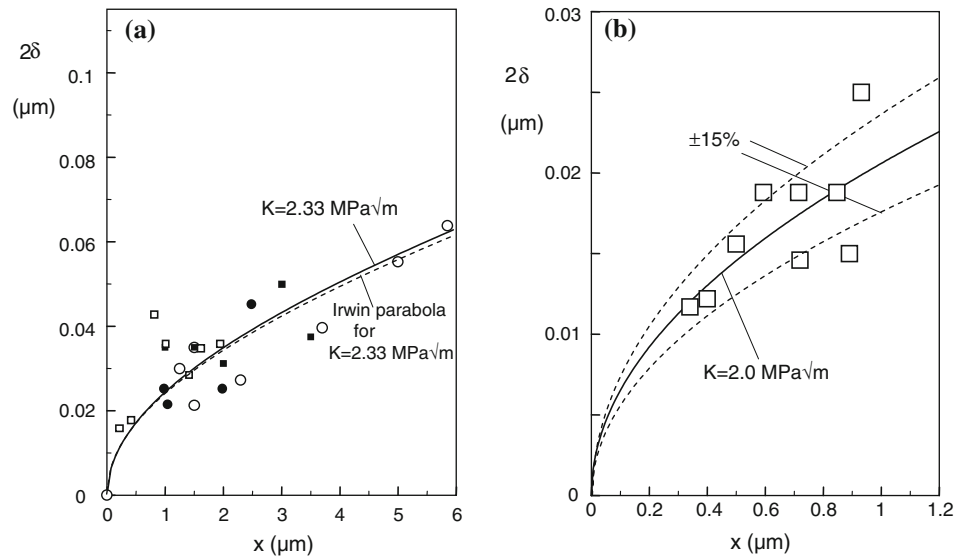
$$E' = \begin{cases} E & \text{for plane stress} \\ E/(1 - \nu^2) & \text{for plane strain} \end{cases} \tag{6}$$

where E is the Young's modulus and ν the Poisson's ratio. Since plane stress prevails at a free surface, it was used $E' = E = 310 \text{ GPa}$.

A representation of the displacement solution Eq. 3 is given in Fig. 2b by the dashed curves. The procedure for the determination of K_{10} may be outlined in detail for material (I). Figure 3a shows a SEM image of a Vickers indentation crack in material (I) very close to the tip. The COD were measured as a function of the distance x from the tips for several cracks. Results are plotted in Fig. 3b as the circles. The solid curve shows an average curve for the experimental data.

For an arbitrarily chosen stress intensity factor of $K = 1 \text{ MPa}\sqrt{\text{m}}$, the displacements were computed for any distance x by using Eqs. 3–5. These values denoted as $2\delta_{\text{comp}}$ are taken in Fig. 4a as the abscissa. From the initially

Fig. 5 **a** Representation of the near-tip displacements for material (I) by a plot $\delta = f(x)$ (solid curve); dashed curve: Irwin parabola according to Eq. 7 for the same stress intensity factor value, and **b** results for material (II)



linear dependency between the measured and the computed displacements, the slope was determined via a least-squares fit with the fitting region $0 \leq 2\delta_{\text{comp}} \leq 0.025 \mu\text{m}$. Figure 4b shows the fitted data in more detail. The different symbols indicate different cracks. A slope of 2.33 was obtained. The dash-dotted straight lines with $\pm 15\%$ deviating slopes border the region in which 66% of the data points are located.

From the slope of 2.33 it can now simply be concluded that the related stress intensity factor in the near-tip region must be $K_{I0} = 2.33 \text{ MPa}\sqrt{\text{m}}$.

Figure 5a shows the final representation of the near-tip data of Fig. 4b with now the (linear) crack-tip distance as the abscissa. The dashed curve represents the so-called Irwin parabola, represented by Eq. 3 for $A_1 = A_2 = 0$, which for $K = K_{I0}$ reads

$$\delta = \sqrt{\frac{8}{\pi} \frac{K_{I0}}{E}} \sqrt{x} \quad (7)$$

Application of the same evaluation procedure to the near-tip displacements for material (II) result in the data of Fig. 5b providing a crack-tip toughness of $K_{I0} = 2.0 \text{ MPa}\sqrt{\text{m}}$ as represented by the solid curve.

Summary

Crack-tip toughness K_{I0} was determined by measurement of crack opening displacement for cracks generated by

Vickers indentation tests for two Si_3N_4 ceramics with (Y_2O_3 , MgO) and (Y_2O_3 , Al_2O_3) additives.

The results were $K_{I0} = 2.33 \text{ MPa}\sqrt{\text{m}}$ for (Y_2O_3 , MgO)-containing and $2.0 \text{ MPa}\sqrt{\text{m}}$ for (Y_2O_3 , Al_2O_3)-containing silicon nitride. Both results are in agreement with the span of literature data for other Si_3N_4 ceramics [1–3] which are within $1.40 \leq K_{I0} \leq 2.7 \text{ MPa}\sqrt{\text{m}}$.

References

1. Pezzotti G, Muraki N, Maeda N, Satou K, Nishida T (1999) J Am Ceram Soc 82:1249
2. Kounga Njiwa AB, Fett T, Rödel J, Quinn GD (2004) J Am Ceram Soc 87:1502
3. Kruzic JJ, Cannon RM, Ager JW III, Ritchie RO (2005) Acta Mater 53:2595
4. Jelitto H, Felten F, Swain MV, Balke H, Schneider GA (2007) J Appl Mech 74:1197
5. Fett T, Fünfschilling S, Hoffmann MJ, Oberacker R, Jelitto H, Schneider GA (2008) J Am Ceram Soc 91:3638
6. Fett T, Kounga Njiwa AB, Rödel J (2005) Eng Fract Mech 72:647
7. Schneider GA, Fett T (2006) J Ceram Soc Jpn 114:1044